Article:
Black, Conor, Chu, Adrian J, Thomas, Gavin H orcid.org/0000-0002-9763-1313 et al. (2 more authors) (2022) Synthesis and antimicrobial activity of an SO2-releasing siderophore conjugate. JOURNAL OF INORGANIC BIOCHEMISTRY. 111875. ISSN 0162-0134

https://doi.org/10.1016/j.jinorgbio.2022.111875

Journal of Inorganic Biochemistry 234 (2022) 111875

Contents lists available at ScienceDirect

Journal of Inorganic Biochemistry

journal homepage: www.elsevier.com/locate/jinorgbio

Synthesis and antimicrobial activity of an SO_2-releasing siderophore conjugate

Conor M. Black [a], Adrian J. Chu [a,b], Gavin H. Thomas [b], Anne Routledge [a], Anne-Kathrin Duhme-Klair [a,c,*]

[a] Department of Chemistry, University of York, York YO10 5DD, UK
[b] Department of Biology, University of York, York YO10 5DD, UK
[c] York Biomedical Research Institute, University of York, York YO10 5DD, UK

ARTICLE INFO

Keywords:
Siderophores
Antimicrobials
Iron uptake
Trojan horse conjugate
SO_2 release
Bioinorganic chemistry

ABSTRACT

A novel Trojan Horse conjugate consisting of an SO_2-releasing 2,4-dinitrobenzenesulfonamide group attached to the monocatecholate siderophore aminochelin was synthesized to examine whether a bidentate catecholate siderophore unit could help potentiate the antimicrobial activity of SO_2-releasing prodrugs. The conjugate obtained displays rapid SO_2 release on reaction with glutathione, and proved more active against *Staphylococcus aureus* than a comparable SO_2-releasing prodrug lacking the siderophore unit, although activity required micromolar concentrations. The conjugate was inactive against wild-type *Escherichia coli*, but activity was observed against an *entA* mutant strain that is unable to produce its major siderophores. Hence, the poor activity of the conjugate in wild-type *E. coli* may be due to the production of native siderophores that can compete with the conjugate for iron binding and uptake.

1. Introduction

A rise in the number of bacterial strains resistant to both front-line treatments and "last resort" antibiotics means there is an urgent need for either the development of new antimicrobial agents with novel modes of action, or the modification of established antimicrobials in order to safeguard activity and extend clinical lifespans. [1–5]

One strategy that has emerged in recent years for the treatment of infection is the design and utilization of prodrugs that can release gaseous molecules with antimicrobial properties, for example nitric oxide (NO) or carbon monoxide (CO). [6–9] These include the recently FDA-approved drugs pretomanid and delamanid (Fig. 1), where the effect of NO release on metabolism in *Mycobacterium tuberculosis* plays a key role in their activity. [10]

Sulfur dioxide (SO_2) has a long history of use as an antimicrobial in food technology, particularly in brewing. [11,12] Despite this, the first report of SO_2-releasing prodrugs as antimicrobial agents was only published in 2012 by Malwal *et al.*, [13] who synthesized a series of 2,4-dinitrobenzenesulfonamide prodrugs that undergo SO_2 release on reaction with biological thiols *via* a nucleophilic aromatic substitution (S_NAr) mechanism (Scheme 1). [13] A number of these prodrugs proved highly effective for treatment of *Mycobacterium tuberculosis*, [13,14] notably benzylamine derivative **1**, which displays comparable activity to the front line TB drug isoniazid. Screening for activity *vs.* Gram-positive bacteria *Staphylococcus aureus* and *Enterococcus faecalis*, and Gram-negative *Escherichia coli* showed less efficacy, particularly in *E. coli*, where no antimicrobial activity was observed. [15]

It is possible that the lack of activity for SO_2-releasing prodrugs like **1**

Abbreviations: AAS, atomic absorption spectroscopy; ATIR, attenuated total reflection infrared spectroscopy; CDI, 1,1′-carbonyldiimidazole; DCM, dichloromethane; DEPT, distortionless enhancement by polarization transfer; DMSO, dimethylsulfoxide; DNS-Cl, 2,4-dinitrobenzenesulfonyl chloride; *E. coli*, *Escherichia coli*; EDC, 1-ethyl-3-(3′-dimethylaminopropyl)carbodiimide; ESI, electrospray ionisation; FA, formic acid; GSH, glutathione; FDA, food and drug administration; HEPES, (4-(2-hydroxyethyl)-1)-piperazineethanesulfonic acid; HPLC, high performance liquid chromatography; HMQC, heteronuclear multiple quantum coherence; HMBC, heteronuclear multiple bond correlation; HRMS, high-resolution mass spectrometry; LB, Lysogney broth; LCMS, liquid chromatography-mass spectrometry; M.p., melting point; NCTC, national collection of type cultures; NMR, nuclear magnetic resonance; NTA, nitrilotriacetic acid; rt, room temperature (20 °C); S_NAr, nucleophilic aromatic substitution; *S. aureus*, *Staphylococcus aureus*; TB, tuberculosis; TFA, trifluoroacetic acid; THF, tetrahydrofuran; TSB, tryptic soy broth; UV–vis, ultraviolet-visible.

* Corresponding author at: Department of Chemistry, University of York, York YO10 5DD, UK.
E-mail address: anne.duhme-klair@york.ac.uk (A.-K. Duhme-Klair).

https://doi.org/10.1016/j.jinorgbio.2022.111875
Received 15 March 2022; Received in revised form 10 May 2022; Accepted 21 May 2022
Available online 26 May 2022

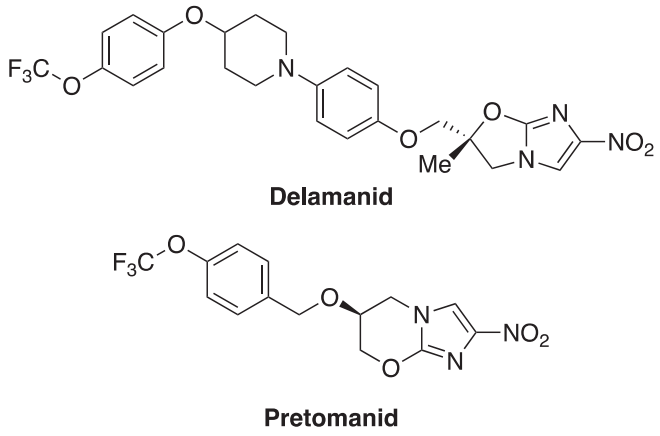

Fig. 1. Structure of FDA-approved antimicrobials delamanid and pretomanid.

against *E. coli* indicates that the prodrugs are unable to permeate both membranes of Gram-negative bacteria, as these provide a significant barrier to a wide range of molecules, including many antibiotics. [16–19] We sought to modulate the uptake of similar SO_2-releasing prodrugs *via* a siderophore-based Trojan Horse approach, since the latter has recently shown promise in the delivery of a variety of antimicrobial compounds. [20–28] The attachment of a siderophore unit to a 2,4-dinitrobenzenesulfonamide prodrug may facilitate uptake of the resulting conjugate *via* iron-siderophore transport pathways in bacteria, thereby bypassing any membrane-associated barriers to uptake.

2. Experimental

2.1. Instrumentation

$^{1}H/^{13}C$ NMR were recorded on JeolECX or JeolECS 400 MHz spectrometers at 298 K. Where necessary, NMR assignments were confirmed using DEPT 135, 2D HMQC (^{1}H-^{13}C single bond) and HMBC (^{1}H-^{13}C multiple bond) correlation experiments. FTIR spectra were recorded using a Perkin-Elmer FT-IR Spectrum Two spectrometer (ATIR). High-resolution mass spectra were recorded on a Thermo-Finnigan LCQ Spectrometer or a Bruker microTOF by Mr. Karl Heaton and Dr. Rosaria Cercola. Elemental analysis was carried out by Dr. Graeme McAllister on an Exeter CE-440 elemental analyzer. UV–vis spectra were recorded on a Shimadzu UV-1800 Spectrophotometer using Starna Scientific quartz cuvettes (3/Q/10 or 21/Q/10, path lengths 1 cm). Uncorrected melting points were recorded using a Stuart Scientific SMP3 instrument.

Preparative HPLC was performed on a Varian ProStar HPLC system with two 210 series pumps (25 mL), a 325 series UV detector, a model 701 fraction collector and a model 410 autosampler using a SunFire Prep C18 column (10 μm, 19 × 250 mm). Preparative LCMS was performed on a Waters LCMS, with a Waters 3100 Mass Detector, Waters 996 Photodiode Array Detector, Waters 2525 Binary Gradient Module, Waters 515 HPLC Pump, Waters SFO (System Fluidics Organiser) and a Waters 2767 Sample Manager using a SunFire Prep C18 column (10 μm, 19 × 250 mm).

Preparative HPLC Method A:

Starting ratio is 40:60 MeCN + 0.1% Formic Acid (FA): H_2O + 0.1% FA. Over 20 min the ratio is increased to 70:30 MeCN + FA: H_2O + FA. The ratio was then reduced to 40:60 MeCN + FA: H_2O + FA for 5 min to re-equilibrate the column. Flow rate 20 mL/min.

Preparative LCMS Method A:

Starting ratio is 50:50 MeCN + 0.1% Formic Acid (FA): H_2O + 0.1% FA. Over 20 min the ratio is increased to 68:32 MeCN + FA: H_2O + FA. The ratio was then reduced to 50:50 MeCN + FA: H_2O + FA for 5 min to re-equilibrate the column. Flow rate 20 mL/min.

2.2. Synthetic methods

2,3-Bis(benzyloxy)benzoic acid (**12**), [29] *N*-(4-Aminobutyl)-2,3-bis(benzyloxy)benzamide hydrochloride (**8**), [30] *N*-(*N*′-*tert*-Butyloxycarbonylethane diamino)-2,3-bis(benzyloxy)benzamide (**13**), [31] *N*-(Aminoethyl)-2,3-bis(benzyloxy)benzamide, TFA salt (**9**), [31] *N*-(4-Aminobutyl)-benzamide (**10**), [32] *N*-Benzyl-2,4-dinitrobenzenesulfonamide (**1**), [13] and *N*-Benzyl-2,4-dinitro-*N*-(prop-2-yn-1-yl)benzenesulfonamide (**18**) [15] were prepared according to literature procedures. Experimental protocols and characterization data are available in the Supporting Information. Compound structures with the atom numbering scheme used for NMR assignments are also available in the Supporting Information.

2.2.1. Synthesis of 2,3-Bis(benzyloxy)-N-(4-(2,4-dinitrobenzenesulfonamido)butyl) benzamide (15)

2,4-Dinitrobenzenesulfonyl chloride (0.147 g, 0.549 mmol) was placed under N_2, then dissolved in dry DCM (25 mL). The solution was cooled to 0 °C, then *N*-(2,3-Bis(benzyloxy)benzoyl)diaminobutane hydrochloride (**8**, 0.221 g, 0.500 mmol) and lutidine (0.25 mL, 2.15 mmol) added. The reaction was stirred at 0 °C for 5 h, and then allowed to warm to room temperature overnight. After stirring for 28 h, water (25 mL) was added and the organic layer separated. The aqueous layer was extracted with DCM (2 × 20 mL), then the combined organic layers were washed with 1 M aq. HCl (40 mL), water (40 mL) and brine (40 mL), dried over $MgSO_4$ and the DCM removed *in vacuo* to give a beige solid (0.312 g, 0.491 mmol, 98%). M.p. = 169–170 °C. R_f = 0.17 (8:1 DCM: EtOAc).

^{1}H NMR: (400 MHz, DMSO-d_6) δ_H ppm: 8.89 (1H, d, *J* = 2.5 Hz, *H28*), 8.62 (1H, dd, *J* = 9.0, 2.5 Hz, *H26*), 8.48 (1H, t, *J* = 6.0 Hz, *H23*), 8.22 (1H, d, *J* = 9.0 Hz, *H25*), 8.16 (1H, t, *J* = 6.0 Hz, *H18*), 7.50–7.49 (2H, m, *Ar H*), 7.43–7.23 (9H, m, *Ar H*), 7.12 (1H, t, *J* = 8.0 Hz, *H3*), 7.08 (1H, dd, *J* = 7.5, 2.0 Hz, *H4*), 5.20 (2H, s, *H8 or 13*), 4.99 (2H, s, *H8 or 13*), 3.13 (2H, app. q, *J* = 6.5 Hz, *H19*), 2.90 (2H, app. q, *J* = 6.5 Hz,

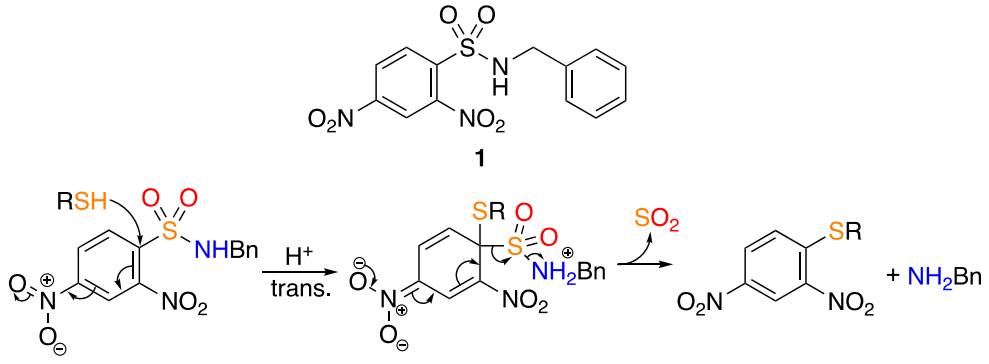

Scheme 1. Structure of SO_2-releasing prodrug **1** (top) and mechanism of SO_2 release on reaction with biological thiols (bottom).

H22), 1.44–1.36 (4H, m, *H20 and 21*).

^{13}C NMR: (100 MHz, DMSO-d_6) δ_C ppm: 165.6 (*C7*), 151.6 (*C5*), 149.6 (*C27*), 147.7 (*C29*), 145.1 (*C6*), 137.8 (*C24*), 137.1, 136.8 (*C9 and 14*), 131.2 (*C25*), 131.1 (*C1*), 128.5, 128.3, 128.2, 128.0, 127.8 (*C10–12 and 15–17*), 127.3 (*C26*), 124.2 (*C3*), 120.7 (*C4*), 120.1 (*C28*), 115.8 (*C2*), 75.1, 70.2 (*C8 and 13*), 42.5 (*C22*), 38.3 (*C19*), 26.6, 26.1 (*C20 and 21*).

HRMS (ESI): Calcd. $[M + H]^+$ ($C_{31}H_{31}N_4O_9S$) $m/z = 635.1806$; Obs. $[M + H]^+$ $m/z = 635.1824$, Mean err −2.2 ppm. Calcd. $[M + Na]^+$ ($C_{31}H_{30}N_4NaO_9S$) $m/z = 657.1626$; Obs. $[M + Na]^+$ $m/z = 657.1642$, Mean err −2.5 ppm.

IR (ATIR, cm^{-1}): 3375 (amide NH stretch, m), 3159 (sulfonamide NH stretch, m), 3130–2870 (C—H stretching, w), 1633 (C═O stretch, s), 1573 (N═O/C═C stretches, m), 1554 (N═O/C═C stretches, s), 1538 (N═O/C═C stretches, s), 1348 (S═O/N═O stretch, s), 1165 (S═O stretch, s).

2.2.2. Synthesis of N-(4-((2,4-Dinitrophenyl)sulfonamido)butyl)-2,3-dihydroxybenzamide (2)

15 (0.200 g, 0.315 mmol) was placed in a 3-necked RBF, then the flask purged with N_2, and dry DCM (7.5 mL) added. Boron tribromide (1 M in DCM, 0.79 mL, 0.790 mmol) was added dropwise and the reaction stirred under flow of N_2 at room temperature for 7 h. Wet methanol (25 mL) was added to quench any remaining BBr_3, then the solvent removed *in vacuo*. MeOH (3 × 15 mL) was added and removed under vacuum, giving an orange-brown solid. The crude product was purified by preparative HPLC chromatography using Prep. HPLC Method A to give **2** as a yellow solid (63.4 mg, 0.140 mmol, 40%). M.p. = 133–134 °C.

^{1}H NMR: (400 MHz, MeCN-d_3) δ_H ppm: 12.99 (1H, s, *H8*), 8.59 (1H, d, $J = 2.0$ Hz, *H20*), 8.48 (1H, dd, $J = 8.5$, 2.0 Hz, *H18*), 8.24 (1H, d, $J = 8.5$ Hz, *H17*), 7.39–7.25 (1H, m, *H10 or 15*), 7.03 (1H, dd, $J = 8.0$, 1.0 Hz, *H2*), 6.96 (1H, dd, $J = 8.0$, 1.0 Hz, *H4*), 6.73 (1H, app. t, $J = 8.0$ Hz, *H3*), 6.55 (1H, br s, *H9*), 6.19 (1H, br t, $J = 6.0$ Hz, *H10 or 15*), 3.31 (2H, app. q, $J = 6.0$ Hz, *H14*), 3.13 (2H, app. q, $J = 6.0$ Hz, *H11*), 1.61–1.49 (4H, m, *H12 and 13*).

^{13}C NMR: (100 MHz, MeCN-d_3) δ_C ppm: 171.2 (*C7*), 151.0 (*C19*), 150.5 (*C6*), 148.9 (*C21*), 146.8 (*C5*), 139.4 (*C16*), 133.1 (*C17*), 128.1 (*C18*), 121.3 (*C20*), 119.2, 119.1 (*C3 and 4*), 117.6 (*C2*), 115.2 (*C1*), 44.0 (*C14*), 39.3 (*C11*), 27.5, 26.9 (*C12 and 13*).

HRMS (ESI): Calcd. $[M + H]^+$ ($C_{17}H_{19}N_4O_9S$) $m/z = 455.0867$; Obs. $[M + H]^+$ $m/z = 455.0869$, Mean err −3.4 ppm. Calcd. $[M + Na]^+$ ($C_{17}H_{18}N_4NaO_9S$) $m/z = 477.0687$; Obs. $[M + Na]^+$ $m/z = 477.0680$, Mean err 1.0 ppm.

IR (ATIR, cm^{-1}): 3527 (OH stretch, w), 3444 (amide NH stretch, w), 3258 (OH stretch – H bonded, w br), 3104 (sulfonamide NH stretch, w), 3100–2850 (C—H stretching, w), 1641 (C═O stretch, m), 1599 (N═O/C═C stretches, m), 1532 (N═O/C═C stretches, s), 1346 (S═O stretch, s), 1333 (N═O stretch, s), 1164 (S═O stretch, s).

2.2.3. Synthesis of 2,3-Bis(benzyloxy)-N-(4-(2,4-dinitrobenzenesulfonamido)ethyl)benzamide (16)

9 (77.9 mg, 0.159 mmol) was dissolved in 1 M aq. NaOH solution (4 mL), and stirred for 30 min, then the solution extracted with DCM (3 × 5 mL), dried over $MgSO_4$ and the solvent removed to give a clear pale yellow oil. The oil was dissolved in anhydrous DCM (10 mL), and the solution cooled to 0 °C, then 2,4-dinitrobenzenesulfonyl chloride (45.6 mg, 0.171 mmol) and lutidine (71 μL, 0.613 mmol) were added, and the reaction was allowed to warm to room temperature and stirred for 24 h. Water (10 mL) was added and the organic layer separated. The aqueous layer was extracted with DCM (2 × 10 mL), then the combined organic layers were washed with 1 M aq. HCl (15 mL), water (20 mL) and brine (15 mL), dried over $MgSO_4$ and the DCM removed *in vacuo* to give a yellow-green oil (83.4 mg, 0.137 mmol, 86%). M.p. = 137–139 °C. R_f = 0.36 (DCM).

^{1}H NMR: (400 MHz, MeOD) δ_H ppm: 8.46 (1H, d, $J = 2.5$ Hz, *H26*), 8.22 (1H, dd, $J = 8.5$, 2.5 Hz, *H24*), 8.11 (1H, d, $J = 8.5$ Hz, *H23*), 7.57–7.54 (2H, m, *Ar H*), 7.45–7.35 (3H, m, *Ar H*), 7.32–7.20 (7H, m, *Ar H*), 7.10 (1H, t, $J = 8.0$ Hz, *H3*), 5.17 (2H, s, *H8 or 13*), 4.99 (2H, s, *H8 or 13*). The peaks for *H19* and *H20* were hidden under the MeOH solvent peak, but were visible on HMQC and HMBC spectra.

^{13}C NMR: (100 MHz, MeOD) δ_C ppm: 167.9 (*C7*), 153.1 (*C5 or 6*), 150.5, 149.0 (*C25 and 27*), 147.4 (*C5 or 6*), 140.8 (*C22*), 138.0, 137.7 (*C9 and 14*), 133.0 (*C23*), 130.1, 129.7, 129.6, 129.4, 129.3 (*C10–12 and 15–17*), 128.0 (*C24*), 127.9 (*C1*), 125.5 (*C3*), 123.0 (*C2*), 121.4 (*C26*), 118.3 (*C4*), 77.2, 72.1 (*C8 and 13*), 44.0, 40.5 (*C19 and 20*).

HRMS (ESI): Calcd. $[M + Na]^+$ ($C_{29}H_{26}N_4NaO_9S$) $m/z = 629.1313$; Obs. $[M + Na]^+$ $m/z = 629.1300$, Mean err 2.8 ppm.

IR (ATIR, cm^{-1}): 3360 (amide NH stretch, w), 3099 (sulfonamide NH stretch, w), 3050–2850 (C—H stretching, w), 1644 (C═O stretch, m), 1575 (N═O/C═C stretches, m), 1537 (N═O/C═C stretches, s), 1454 (N═O/C═C stretches, s), 1346 (S═O stretch, s), 1165 (S═O stretch, s).

2.2.4. Synthesis of N-[2-(2,4-Dinitrobenzenesulfonamido)ethyl]-2,3-dihydroxybenzamide (5)

16 (0.118 g, 0.195 mmol) was dissolved in dry DCM (5 mL) and placed in a 3-necked RBF, then the flask purged with N_2. Boron tribromide (1 M in DCM, 0.488 mL, 0.488 mmol) was added dropwise and the reaction stirred under flow of N_2 at room temperature overnight. Extra DCM (5 mL) was added in the morning as the reaction had almost dried out. Wet methanol (25 mL) was added to quench any remaining BBr_3, then the solvent removed *in vacuo*. MeOH (3 × 20 mL) was added and removed under vacuum, giving a yellow-orange oil. The crude product was purified by preparative LCMS chromatography using Prep. LCMS Method A to give a yellow solid (45.6 mg, 0.107 mmol, 55%). M.p. = 175–177 °C.

^{1}H NMR: (400 MHz, MeCN-d_3) δ_H ppm: 12.59 (1H, br s, *H8*), 8.45 (1H, d, $J = 2.0$ Hz, *H18*), 8.32 (1H, dd, $J = 8.5$, 2.5 Hz, *H16*), 8.18 (1H, d, $J = 8.5$ Hz, *H15*), 7.41 (1H, br s, *H10 or 13*), 6.88 (1H, d, $J = 8.0$ Hz, *H4*), 6.84 (1H, d, $J = 8.0$ Hz, *H2*), 6.66 (1H, app. t, $J = 8.0$ Hz, *H3*), 6.60–6.30 (2H, m, *H9 and H10 or 13*), 3.50–3.40 (4H, m, *H11 and 12*).

^{13}C NMR: (100 MHz, MeCN-d_3) δ_C ppm: 171.5 (*C7*), 150.39, 150.36 (*C6 and 17*), 148.6 (*C19*), 146.7 (*C5*), 139.7 (*C14*), 132.8 (*C15*), 128.2 (*C16*), 121.2 (*C18*), 119.5 (*C4*), 119.3 (*C3*), 117.7 (*C2*), 114.7 (*C1*), 43.9, 39.7 (*C11 and 12*).

HRMS (ESI): Calcd. $[M + Na]^+$ ($C_{15}H_{14}N_4NaO_9S$) $m/z = 449.0374$; Obs. $[M + Na]^+$ $m/z = 449.0376$, Mean err −1.1 ppm.

IR (ATIR, cm^{-1}): 3436 (OH stretch, m), 3407 (amide NH stretch, m), 3114 (sulfonamide NH stretch, w), 3110–2850 (C—H stretching, w), 1639 (C═O stretch, m), 1599 (N═O/C═C stretches, m), 1546 (N═O/C═C stretches, s), 1534 (N═O/C═C stretches, s), 1346 (S═O stretch, s), 1336 (N═O stretch, s), 1163 (S═O stretch, s).

2.2.5. Synthesis of N-[4-(2,4-Dinitrobenzenesulfonamido)butyl]benzamide (6)

2,4-Dinitrobenzenesulfonyl chloride (0.157 g, 0.590 mmol) was placed under N_2, then dissolved in dry DCM (10 mL). The solution was cooled to 0 °C, then **10** (0.107 g, 0.555 mmol) was dissolved in in dry DCM (10 mL) and added. Lutidine (0.26 mL, 2.23 mmol) was then added, and the reaction was allowed to warm to room temperature and stirred for 24 h. As the reaction had not gone to completion, extra sulfonyl chloride (0.02 g, 0.07 mmol) and lutidine (0.08 mL, 0.69 mmol) were added and the reaction stirred for an additional 72 h. Water (20 mL) was added and the organic layer separated. The aqueous layer was extracted with DCM (2 × 20 mL), then the combined organic layers were washed with 1 M aq. HCl (35 mL), water (30 mL) and brine (30 mL), dried over $MgSO_4$ and the DCM removed *in vacuo* to give a viscous orange oil, which solidified overnight to form a brown solid (0.112 g, 0.264 mmol, 48%). M.p. = 145 °C.

^{1}H NMR: (400 MHz, MeOD) δ_H ppm: 8.68 (1H, d, $J = 2.5$ Hz, *H16*), 8.55 (1H, dd, $J = 8.5$, 2.5 Hz, *H14*), 8.31 (1H, d, $J = 8.5$ Hz, *H13*), 7.77 (2H, dt, $J = 7.0$, 1.5 Hz, *H2*), 7.53 (1H, tt, $J = 7.0$, 1.5 Hz, *H4*), 7.45 (2H, tt, $J = 7.0$, 1.5 Hz, *H3*), 3.35 (2H, t, $J = 7.0$ Hz, *H7*), 3.16 (2H, t, $J = 7.0$

Hz, *H10*), 1.69–1.54 (4H, m, *H8 and 9*).

^{13}C NMR: (100 MHz, MeOD) δ_C ppm: 170.2 (*C5*), 151.3, 149.5 (*C15 and 17)*, 140.3 (*C12),* 135.7 (*C1*), 133.2 (*C13*), 132.6 (*C4*), 129.6 (*C3*), 128.2 (*C2*), 127.9 (*C14*), 121.4 (*C16*), 44.1 (*C10*), 40.2 (*C7*), 28.3, 27.6 (*C8 and 9*).

HRMS (ESI): Calcd. $[M + H]^+$ ($C_{17}H_{19}N_4O_7S$) *m/z* = 423.0969; Obs. $[M + H]^+$ *m/z* = 423.0967, Mean err −0.3 ppm. Calcd. $[M + Na]^+$ ($C_{17}H_{18}N_4NaO_7S$) *m/z* = 445.0788; Obs. $[M + Na]^+$ *m/z* = 445.0784, Mean err 1.1 ppm.

IR (ATIR, cm^{-1}): 3452 (amide NH stretch, w), 3159 (amide NH stretch II, w br), 3105 (sulfonamide NH stretch, w), 3050–2800 (C═H stretching, w), 1654 (C═O stretch, s), 1603 (N═O/C═C stretches, w), 1580 (N═O/C═C stretches, w), 1550 (N═O/C═C stretches, s), 1524 (N═O/C═C stretches, s), 1361 (N═O stretch, s), 1343 (S═O stretch, s), 1164 (S═O stretch, s).

2.2.6. Synthesis of 2,3-Bis(benzyloxy)-N-{4-[(2,4-dinitrophenyl)amino] butyl}benzamide (17)

8 (0.109 g, 0.247 mmol) was placed under N_2, then dissolved in dry DCM (6 mL). 1-Chloro-2,4-dinitrobenzene (50.9 mg, 0.251 mmol) and Et_3N (0.105 mL, 0.753 mmol) were added, and the resulting yellow solution was stirred at room temperature for 24 h. Extra DCM (5 mL) and water (10 mL) were added and the layers separated. The aqueous layer was extracted with DCM (2 × 10 mL), then the combined organic layers were washed with 1 M aq. HCl (15 mL), water (15 mL), 1 M $NaHCO_3$ solution (5 mL) and brine (15 mL), dried over $MgSO_4$ and the DCM removed *in vacuo*. The crude product was purified by column chromatography (silica gel, 2:1 EtOAc:40–60 °C pet. ether) to give **17** as a yellow-orange glassy solid (92.0 mg, 0.161 mmol, 65%). M.p. = 113–114 °C. R_f = 0.71 (EtOAc); 0.62 (9:1 DCM:MeOH); 0.31 (2:1 EtOAc:40–60 °C pet. ether).

^{1}H NMR: (400 MHz, DMSO-d_6) δ_H ppm: 8.85–8.82 (2H, m*, H23 and 28*), 8.24–8.18 (2H, m*, *H18* and *26*), 7.51–7.48 (2H, m, *Ar H*), 7.43–7.31 (5H, m, *Ar H*), 7.29–7.25 (4H, m, *Ar H*), 7.17 (1H, d, *J* = 10.0 Hz, *H25*), 7.12 (1H, t, *J* = 8.0 Hz, *H3*), 7.08 (1H, dd, *J* = 8.0, 2.0 *Hz, H2 or 4)*, 5.20 (2H, s, *H8 or 13*), 4.99 (2H, s, *H8 or 13*), 3.43 (2H, app. q, *J* = 6.5 Hz, *H22*), 3.24 (2H, app. q, *J* = 6.5 Hz, *H19*), 1.63–1.46 (4H, m, *H20 and 21*).

* t and dd overlapping.

^{13}C NMR: (100 MHz, DMSO-d_6) δ_C ppm: 165.7 (*C7*), 151.6 (*C5*), 148.1 (*C27*), 145.1 (*C6*), 137.1, 136.8 (*C9 and 14*), 134.6 (*C1*), 131.3 (*C24*), 129.9 (*C26*), 129.6 (*C29*), 128.5, 128.23, 128.16, 128.02, 127.97, 127.8 (*C10–12 and 15–17*), 124.2, 123.7 (*C28 and C2 or 4*), 120.7 (*C3*), 115.7, 115.3 (*C25 and C2 or 4*), 75.1, 70.1 (*C8 and 13*), 42.3 (*C22*), 38.6 (*C19*), 26.3, 25.5 (*C20 and 21*).

HRMS (ESI): Calcd. $[M + H]^+$ ($C_{31}H_{31}N_4O_7$) *m/z* = 571.2187; Obs. $[M + H]^+$ *m/z* = 571.2192, Mean err −1.1 ppm. Calcd. $[M + Na]^+$ ($C_{31}H_{30}N_4NaO_7$) *m/z* = 593.2007; Obs. $[M + Na]^+$ *m/z* = 593.2015, Mean err −0.2 ppm. Calcd. $[M + K]^+$ ($C_{31}H_{30}KN_4O_7$) *m/z* = 609.1746; Obs. $[M + K]^+$ *m/z* = 609.1749, Mean err −1.0 ppm.

IR (ATIR, cm^{-1}): 3376 (amide NH stretch, m), 3115–2875 (C═H stretching, w), 1651 (C═O stretch, s), 1617 (N═O/C═C stretches, s), 1586 (N═O/C═C stretches, s), 1575 (N═O/C═C stretches, s), 1520 (N═O/C═C stretches, s), 1336 (N═O stretch, s).

2.2.7. Synthesis of N-{4-[(2,4-Dinitrophenyl)amino]butyl}-2,3-dihydroxybenzamide (7)

17 (0.067 g, 0.117 mmol) was placed in a 3-necked RBF, then the flask purged with N_2, and dry DCM (3.5 mL) added. Boron tribromide (1 M in DCM, 0.40 mL, 0.400 mmol) was added dropwise and the reaction stirred at room temperature for 22 h. Wet methanol (15 mL) was added to quench any remaining BBr_3, then the solvent removed *in vacuo*. MeOH (3 × 15 mL) was added and removed under vacuum, giving an orange-black solid. The crude product was purified by preparative HPLC chromatography using Prep. LCMS Method A to give **7** as a brown solid (9.9 mg, 0.025 mmol, 22%).

^{1}H NMR: (400 MHz, DMSO-d_6) δ_H ppm: 12.80 (1H, s, *H8*), 9.13 (1H, br s*, H9*), 8.91 (1H, br t, *J* = 6.0 Hz, *H10 or 15*), 8.84 (1H, d, *J* = 2.5 Hz, *H20*), 8.80 (1H, br t, *J* = 6.0 Hz, *H10 or 15*), 8.23 (1H, dd, *J* = 9.5, 2.5 Hz, *H18*), 7.26–7.22 (2H, m, *H17 and H2 or 4*), 6.88 (1H, dd, *J* = 8.0, 2.0 Hz, *H2 or 4*), 6.64 (1H, t, *J* = 8.0 Hz, *H3*), 3.53 (2H, app. q, *J* = 6.0 Hz, *H14*), 3.37–3.20 (2H, m, *H11*), 1.71–1.59 (4H, m, *H12 and 13*).

HRMS (ESI): Calcd. $[M + H]^+$ ($C_{17}H_{19}N_4O_7$) *m/z* = 391.1248; Obs. $[M + H]^+$ *m/z* = 391.1251, Mean err −0.7 ppm.

2.3. SO_2 release studies

1 mM stock solutions of the compounds for SO_2 release study were made up in MeCN. Other stock solutions were prepared as follows:

HEPES Buffer 20 mm pH 7.4

HEPES buffer was made fresh every three months. The pH of a stock solution of 100 mM HEPES was adjusted to pH 7.4 by addition of aqueous sodium hydroxide, then diluted to 20 mM.

Glutathione

10 mM stock solutions of glutathione in 20 mM HEPES buffer (pH 7.4) were made fresh before every experiment, and the stocks renewed daily.

Dye 20

A 1 mM stock of SO_2-releasing dye **20** was made up in MeCN *via* a 10-fold dilution from a 10 mM stock. A new stock was made up every 6 months.

Fe(NTA) Solution

Nitrilotriacetic acid trisodium salt (0.1 mmol) was dissolved in AAS absorption standard $Fe(NO_3)_3$ solution (0.0179 M, 5.587 mL). This solution was made up to 10 mL with milliQ H_2O, to give a final solution containing 0.01 M $Fe(NO_3)_3$ and 0.01 M NTA.

SO_2 release experiments were carried out in quartz cuvettes. First, a 100 μM solution of the desired conjugate was made up from 250 μL conjugate stock solution (1 mM) + 2250 μL HEPES, and used to record a baseline on the on the UV–vis spectrometer. A second solution of the conjugate was made up from 250 μL 1 mM stock solution +2000 μL HEPES buffer. 250 μL 10 mM GSH was then added, and the solution mixed quickly *via* pipette, before being transferred to the UV–vis spectrometer for measurement of the absorption spectra at regular time intervals.

For experiments with dye **20**, a baseline cuvette was made up from 250 μL conjugate (1 mM) + 2225 μL HEPES buffer +25 μL MeCN, and a reaction cuvette from 250 μL conjugate (1 mM) + 1975 μL HEPES buffer +25 μL dye **20** (1 mM) + 250 μL GSH. For experiments with iron-bound conjugate, a baseline stock solution was made up from 250 μL conjugate (1 mM) + 2225 μL HEPES buffer +25 μL 3.33 mM Fe(NTA), and a reaction solution from 250 μL conjugate (1 mM) + 1975 μL HEPES buffer +25 μL 3.33 mM Fe(NTA) + 250 μL GSH.

2.4. Biological studies

2.4.1. Preparation of media

Stock solutions of **2**, **7** and **18** were made up in MeCN, and a stock solution of aminochelin was made up in DMSO. All other solutions and media were prepared using distilled H_2O (dH_2O) and sterilised by autoclave or filter sterilisation prior to use. The antibiotic kanamycin was added when required to select for mutant strains. For undefined rich media, TSB and LB solids were purchased from commercial sources and used as directed. A chemically-defined M9 Minimal Medium was prepared from stock solutions of commercial SigmaAldrich 5× M9 salts, 20% glucose, 1 M $MgSO_4$, and 1 M $CaCl_2$. 10% casamino acids can also be added. For Chelex-treated M9 media, 5% *w/v* Chelex resin was stirred with each stock solution for 1 h, before passing through a 0.22 μM pore cellulose acetate membrane bottle-top vacuum filtration system (Corning, New York, USA).

Working under defined conditions: For both cell-containing M9-based overnight starter cultures, final inoculum and cell-free M9 media

Table 1
Stock solutions and volumes used for preparation of a 20 mL working stock of M9 media, where dH_2O may be deducted to make room for defined bacterial suspensions or other supplements as required.

Stock Solutions (autoclaved or filter-sterilised)	Volume
dH_2O	14.725 mL
5× M9 Salts	4 mL
(Optional: 10% casamino acids)	(800 µL)
20% glucose	400 µL
1 M $MgSO_4$	40 µL
1 M $CaCl_2$	2 µL
(Optional for mutant: 30 mg/mL kanamycin)	33.33 µL (for 50 µg/mL final)

controls, a total volume of 20 mL each was prepared and used to either inoculate or load their respective wells in 96-well plates for bacterial growth curve experiments.

A 20 mL working stock of M9 media was made up as shown in Table 1:

Composition of M9-based final inoculum: A sterile conical flask containing the M9 components in their requisite volumes was made up, then a preliminary volume of dH_2O (10.725 mL) added. A 1 mL homogenised suspension of the overnight starter culture (see Section 2.4.2) was taken and transferred into a 1 mL Kartell cuvette and the OD_{600} measured using a Jenway spectrophotometer or the cuvette mode of the Epoch 2 plate reader (BioTek, Vermont, USA); if this value exceeded the dynamic range of the instrument, the culture was diluted by 20-fold, then the resulting value multiplied to give the extrapolated OD_{600} of the starter culture. From this OD_{600} value, the volume of starter culture required to give an OD_{600} of 0.05 in the inoculum was calculated, and this volume taken and added to the M9-containing flask. The resulting suspension was then made up to 20 mL with dH_2O. Other additives *e.g.* Fe(NTA) can be added in place of an equivalent volume of dH_2O.

2.4.2. Bacterial growth assays

Starter cultures for bacterial growth curve experiments were prepared by making up 20 mL of the selected media (defined or undefined) in a sterile 125 mL conical flask, followed by inoculation with partially thawed bacterial glycerol stocks. Inoculation was carried out by either directly pipetting 10 µL of the glycerol stock into the starter culture, or by dipping a 10 µL loop from the glycerol stocks into the culture. The cultures were incubated overnight at 37 °C with agitation at 200 rpm.

Growth assays were carried out in 96-well plates using an Epoch 2 plate reader (BioTek, Vermont, USA). A final inoculum was made up for the selected bacteria and media as detailed above (for M9-based work see Section 2.4.1). Wells were made up to a total volume of 200 µL, and no more than 2% organic solvents; both the moats (1.7 mL per quadrant) and the edge wells (200 µL) were filled with dH_2O. Control wells consisted of blank media (cell-free, 200 µL) or final inoculum (drug-free, 200 µL); a solvent control containing final inoculum (196 µL) and the solvent used for the test compound (4 µL) was also set up. For sample wells, final inoculum (196 µL) was added, then 4 µL of test compound stock solutions were added, respectively. The plates were incubated at 37 °C and shaken continuously in a double orbital pattern, where OD_{600} was recorded initially after 5 s, then at half-hourly intervals for the following 24 h.

3. Results and discussion

3.1. Compound design

Initially, a simple conjugate (**2**) based on the monocatechol siderophore aminochelin was envisaged (Fig. 2). The use of a monocatechol was in part inspired by the success in clinical trials of the Trojan Horse antimicrobial cefiderocol (Fig. 2), which contains a monocatechol unit and displays activity against a number of Gram-negative species. [33–35]

Two previous aminochelin-based conjugates in the literature have shown reasonable activity against their target bacteria (Fig. 3), [36,37] including oxazolidinone conjugate **4**, which displayed 8× higher activity against *Pseudomonas aeruginosa* compared to the parent antibiotic. [37] This is notable as the parent oxazolidinone is inactive against Gram-negative bacteria due to poor membrane permeability.

Two additional SO_2-releasing conjugates, an analogue of target compound **2** containing a 2-carbon linker (**5**), and catechol-free conjugate (**6**), were designed to probe the effects of linker length and the presence of the iron-binding catechol group on the rate of SO_2 release from the conjugates. In addition, compound **7**, a close structural analogue of **2** that lacks the ability to release SO_2, was designed as a control for biological experiments. The latter will help to determine whether any antimicrobial activity observed stems from SO_2 release, or from the underlying chemical structure of the conjugate (Fig. 4).

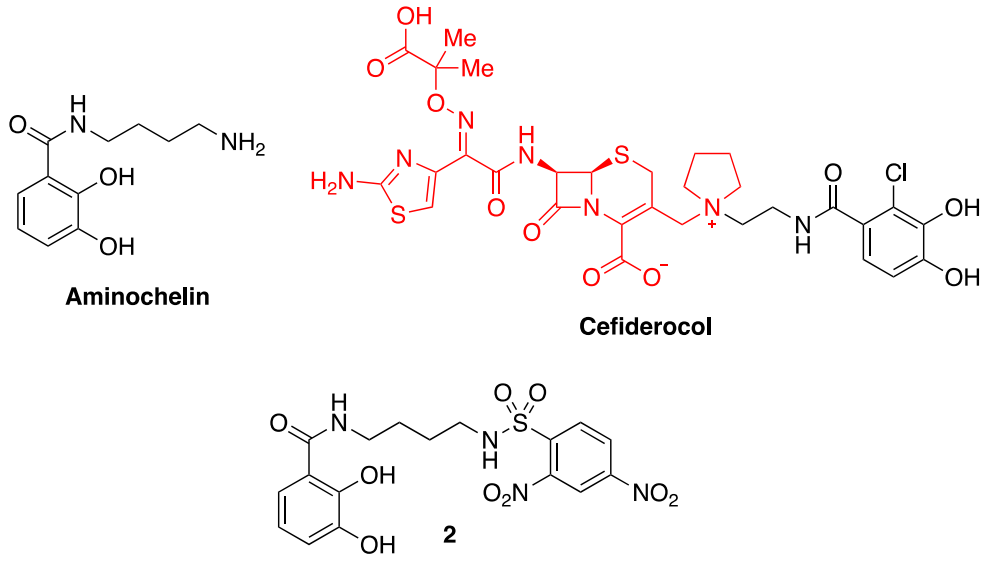

Fig. 2. Structures of monocatechol siderophore aminochelin, Trojan Horse antimicrobial cefiderocol, and 2,4-dinitrobenzenesulfonamide conjugate **2** (antimicrobial unit highlighted in red).

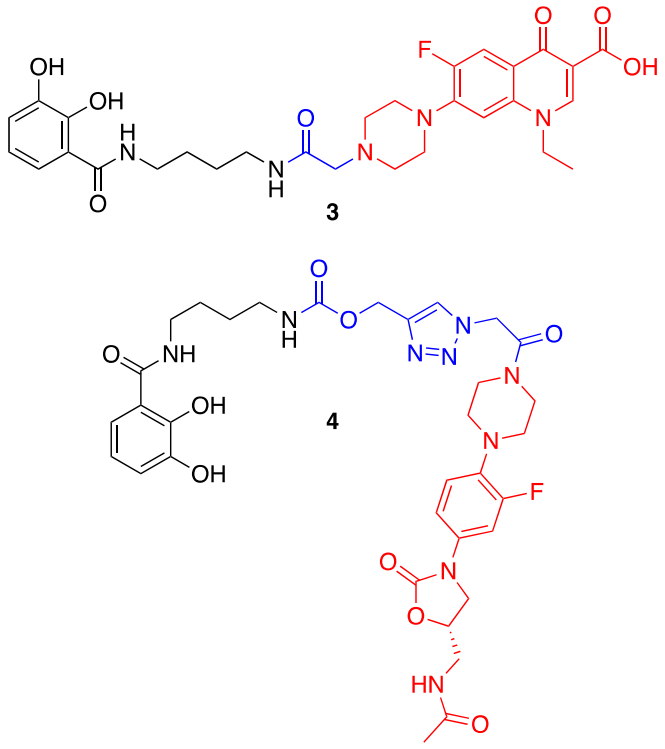

Fig. 3. Previously reported Trojan Horse conjugates utilizing aminochelin as a siderophore component (antimicrobial unit highlighted in red).

3.2. Synthesis

The amine components required for the preparation of the targeted sulfonamides were synthesized according to literature procedures (benzyl-protected aminochelin **8** [30], **9** [31] and **10** [32], Scheme 2).

Installation of the 2,4-dinitrobenzenesulfonamide units for SO_2 release was achieved by reaction of the corresponding amines with commercially-available 2,4-dinitrobenzenesulfonyl chloride (DNS-Cl) to give **6**, **15** and **16**. Conjugates **2** and **5** were obtained following BBr_3-mediated deprotection of **15** and **16** (Scheme 3).

Control compound **7** was synthesized *via* an S_NAr reaction of **8** with 1-chloro-2,4-dinitrobenzene, followed by BBr_3-mediated removal of the benzyl groups (Scheme 4). Finally, the synthesis of previously-reported prodrugs **1** and **18** was carried out from benzylamine (**19**) according to the literature (Scheme 4). [13,15]

3.3. SO_2 release

Qualitative identification of SO_2 release from the synthesized sulfonamides was confirmed *via* their reaction with glutathione (GSH) in aqueous buffer (10% MeCN in HEPES) in the presence of a SO_2-detecting dye, **20**. On reaction with sulfite, formed from SO_2 release in aqueous solution, the dye undergoes a colorimetric change from pink to yellow, which can be followed by UV–vis spectroscopy. The rate of SO_2 release from the synthesized conjugates was determined by observing the formation of the 2,4-dinitrobenzene-GSH conjugate (**21**, Scheme 5) *via* UV–vis spectroscopy; the conjugate exhibits a well-defined UV–vis absorption band at 340 nm (extinction coefficient: 10500 M^{-1} cm^{-1}). [38,39]

Benzylamine conjugate **1**, aminochelin conjugate **2** and catechol-free conjugate **6**, all display similar SO_2 release rates, with the majority of release taking place within the first hour. Comparison of the release rates of **2** and **6** suggests the catechol groups of aminochelin have a small negative effect on the rate of SO_2 release. Compound **5**, with its shorter 2-carbon linker between the catechol and 2,4-dinitrobenzenesulfonamide groups, displays a drastically reduced release rate. Given the shorter linker length between the catechol and the dinitrobenzene ring in **5**, it is possible that there is some form of intramolecular interaction between these two rings, whether in the form of pi-pi stacking, or in the form of hydrogen bonding between the substituents. This could have the effect of hindering the nucleophilic attack of glutathione on the sulfonamide (Fig. 5).

SO_2 release from **2** and **5** was also probed in the presence of Fe(III) to examine the effects of iron coordination on the rate of SO_2 release. One equivalent of Fe(III) was added for every three equivalents of ligand to try to favor the formation of a tris-catecholate complex. On addition of Fe(III) to a solution of **2** or **5**, a purple-blue color forms, suggesting the formation of an iron complex. A clear increase in release rate for the iron-bound conjugates is observed in both cases (Fig. 6).

3.4. Biological screening

3.4.1. S. aureus

Three compounds were selected for investigation of their antimicrobial properties: aminochelin conjugate **2**, control compound **7** and prodrug **18**. The compounds were first screened against a strain of *S. aureus* (NCTC 6571). Prodrug **18** has previously displayed efficacy against two strains of *S. aureus*. [15] Growth assays were carried out in nutrient-rich Tryptic Soy Broth (TSB) in 96-well plates. [40] Growth inhibition is observed at high concentrations (50 to 500 μM) of **2** and **18**, although with notable loss of activity over time for all concentrations apart from 500 μM **2** (Fig. 7). No activity was observed for **7**. The

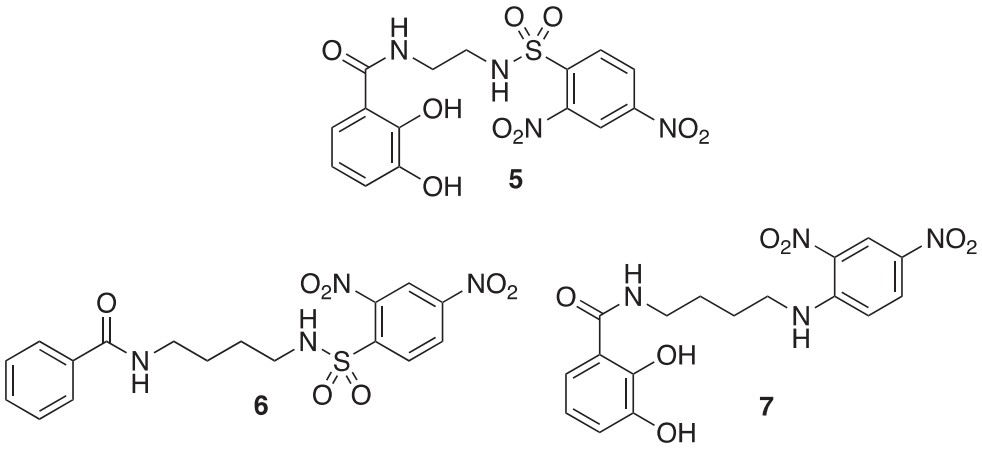

Fig. 4. Structures of sulfonamide analogues designed to probe the nature of SO_2 release and antimicrobial activity.

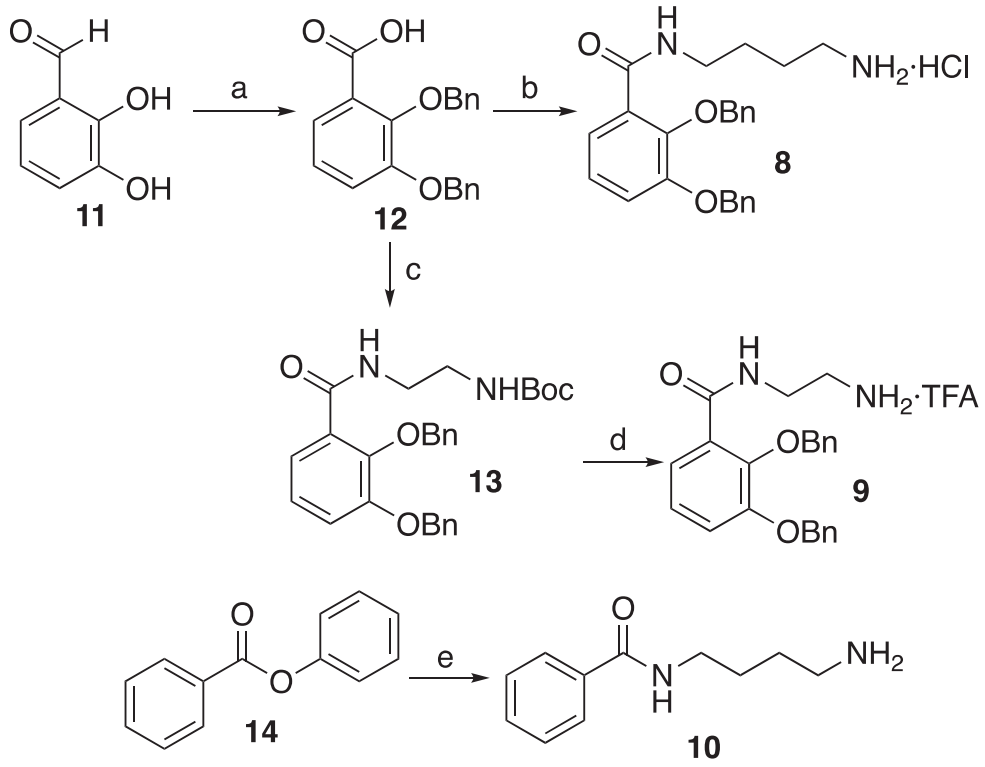

Scheme 2. Synthesis of amine components. a) 1) BnCl, K_2CO_3, EtOH, reflux, 24 h; 2) Sodium chlorite, sulfamic acid, acetone:H_2O (5:4), 2 h, 67% over two steps; b) 1,4-diaminobutane, CDI, THF, 22 h, 38%; c) *N*-Boc ethylenediamine, EDC.HCl, HOBt, DCM, 24 h, 88%; d) TFA (10% *v*/v), DCM, 4 h, 77%; e) 1,4-Diaminobutane, H_2O, N_2, 50 °C, 24 h, 60%.

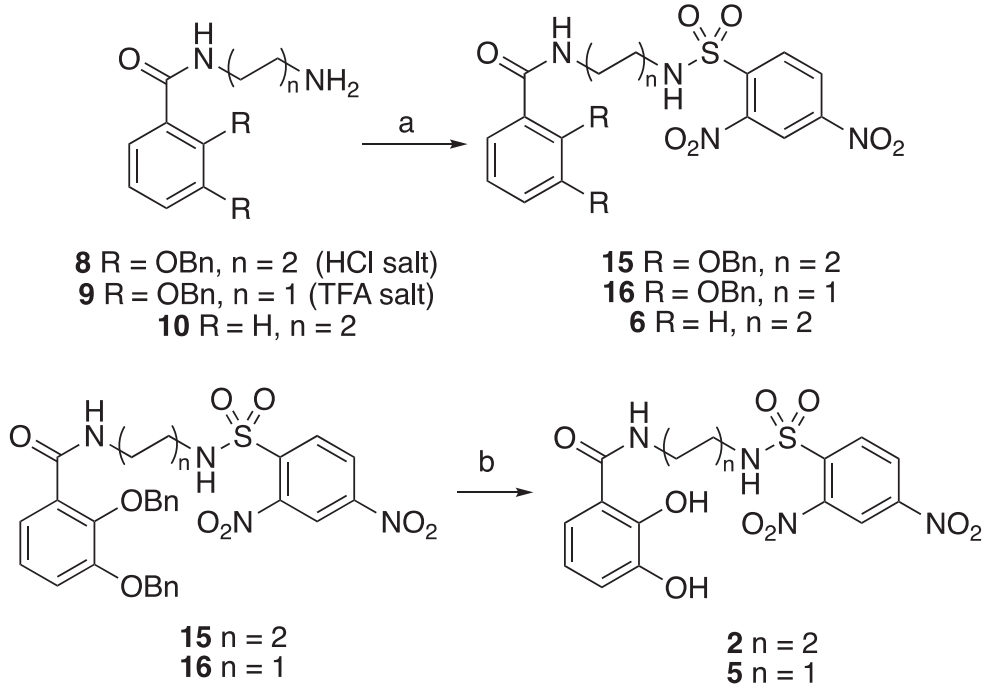

Scheme 3. Synthesis of 2,4-dinitrobenzenesulfonamide conjugates **2**, **5**, and **6.** a) 2,4-Dinitrobenzenesulfonyl chloride, lutidine, DCM (anhydrous), 0 °C to rt., 20–96 h, 48–98%; b) BBr_3, DCM (anhydrous), rt., 7–24 h, 40–55%.

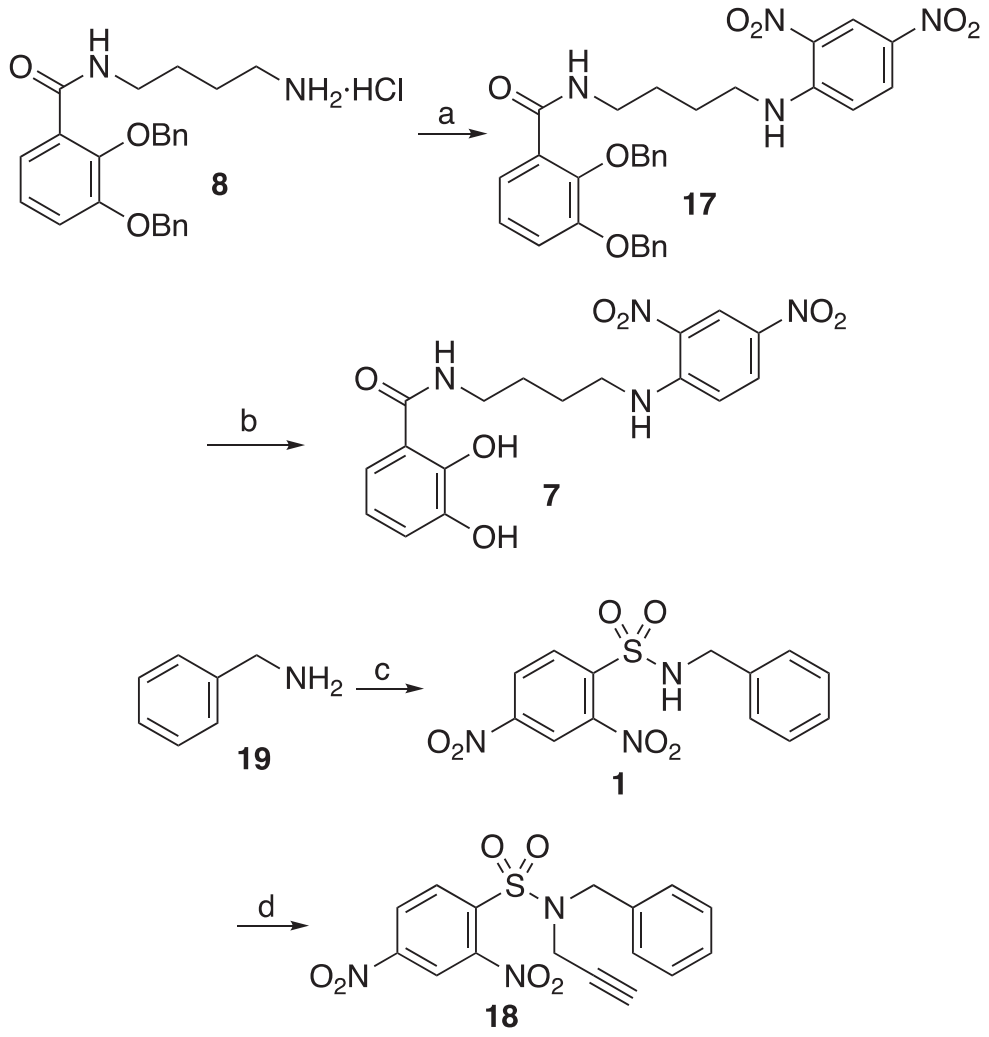

Scheme 4. Synthesis of compound **7** and Chakrapani's prodrugs **1** and **18**. a) 1-Chloro-2,4-dinitrobenzene, Et_3N, DCM (anhydrous), 18 h, 71%; b) BBr_3, DCM (anhydrous), N_2, 22 h, 22%; c) Benzylamine, pyridine, DCM (anhydrous), 0 °C to rt., 24 h, 65%; d) propargyl bromide, K_2CO_3, DMF, rt., 24 h, 68%.

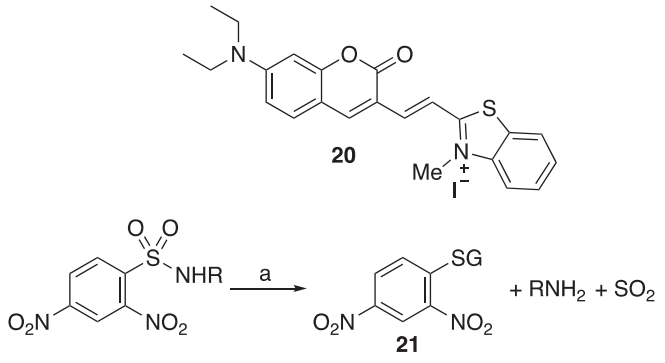

Scheme 5. Structure of SO_2-detecting dye **20** and products of the reaction between 2,4-dinitrobenzenesulfonamide prodrugs and glutathione. a) GSH (10 eq.), 10% MeCN:HEPES, pH 7.4, rt., 12 h.

antimicrobial activity of **2** is improved compared to **18**, potentially indicating that the aminochelin unit is able to facilitate better uptake into the cells, and therefore the release of more SO_2. The shape of the growth curves differs from the typical sigmoidal curves observed for bacterial growth. [41] A biphasic growth curve can indicate a change in the metabolism of the bacteria, [42] or indicate that the bacteria are able to tolerate the presence of an antimicrobial, and even overcome it completely, and it is not exactly clear where the bacteria display these growth kinetics. [43,44] Extracts from wells containing 500 μM of **2** displayed growth when spread out on an agar plate, indicating bacteriostatic rather than bactericidal behavior (Fig. S1).

3.4.2. *E. coli*

The compounds were also screened in an analogous fashion for their activity against *E. coli*. Screening was first carried out in nutrient-rich LB media, with all three compounds displaying no activity over 24 h (Fig. 8). For aminochelin conjugate **2**, this could suggest a high abundance of iron in the media making the expression of outer membrane transporters unnecessary. Outer membrane transporters for iron-siderophores are generally not present in iron-rich conditions. [45] In addition, native siderophores with higher affinity for iron could be present, and these could outcompete **2** for iron binding, thereby preventing uptake.

Screening was then carried out in M9 media supplemented with casamino acids. This nutrient-poor and well-defined media was intended to provide an iron-poor environment, which would better mimic the iron-poor growth conditions that would be present in the host organism, and lead to greater expression of bacterial outer membrane transporters for iron-siderophores, and hence improved uptake of **2**. As with LB media, all three conjugates proved inactive (Fig. 8). Again, it is possible that **2** is outcompeted for iron binding by the high-affinity native

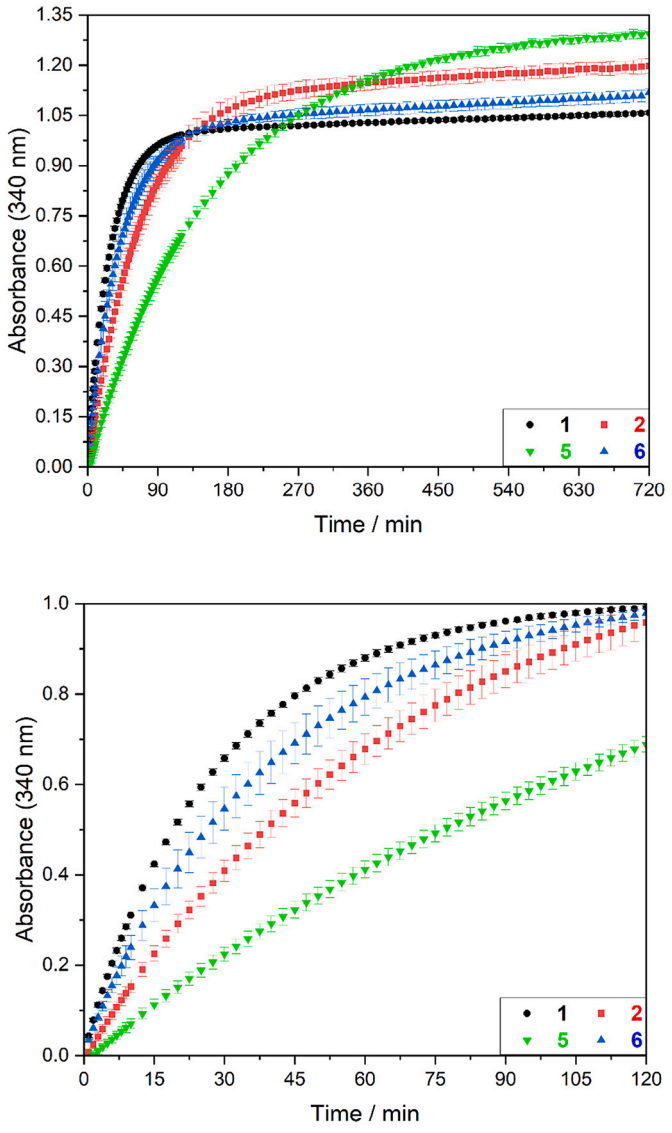

Fig. 5. SO_2 release from 2,4-dinitrobenzenesulfonamide prodrugs on reaction with 10 eq. of glutathione in HEPES buffer (pH 7.4) over 12 h (top) and 2 h (bottom), respectively.

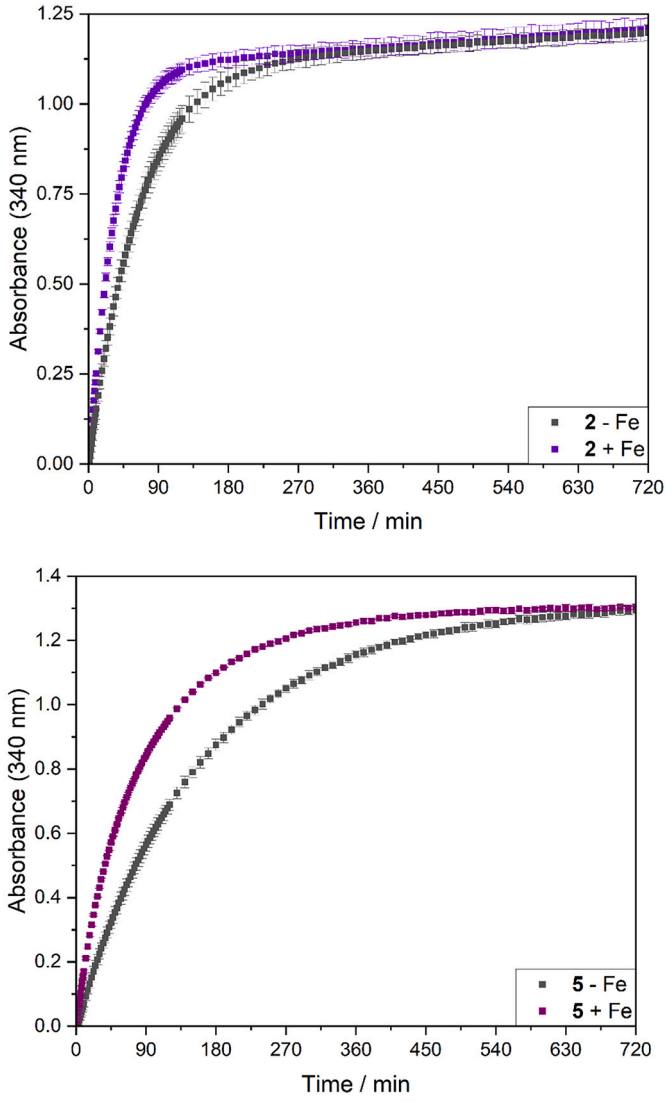

Fig. 6. Plots of absorbance at 340 nm *vs.* time for conjugates **2** (top) and **5** (bottom) on reaction with glutathione (10 eq.) in HEPES buffer (pH 7.4) in the presence and absence of 0.33 eq. Fe(III).

siderophores of *E. coli*.

To examine whether the lack of antimicrobial activity *vs. E. coli* comes from **2** being outcompeted by native siderophores, analogous assays on an *entA*-deficient strain of *E. coli*, JW0588-1, were carried out. This strain lacks the gene for production of the EntA enzyme, which is responsible for catalyzing the final step in the biosynthesis of 2,3-dihydroxybenzoic acid from chorismate. [46,47] As all of the catechol-type siderophores produced by *E. coli* stem from 2,3-dihydroxybenzoic acid, the mutant should be unable to produce and secrete native siderophores that can compete with **2**.

2 was screened against the *entA* mutant in M9 cultures grown with and without casamino acids present. No activity was observed for the *entA* mutant in the casamino acid culture, but when **2** is screened against cultures in plain M9, growth inhibition can be observed at 250 μM and 50 μM, suggesting that in the absence of siderophores in these conditions **2** can be taken up and provide an antimicrobial effect (Fig. 9). Compound **7** and the parent siderophore aminochelin are inactive against the *entA* mutant under the same conditions (**Figs. S2/S3**). This indicates that the antimicrobial activity observed for compound **2** *vs.* the *entA* mutant is unlikely to stem from the chelation properties of the siderophore unit. Compound **18** also proved inactive against the *entA* mutant, suggesting the activity is related to uptake in the absence of siderophores rather than a general increase in SO_2 susceptibility or membrane permeability in the mutant strain.

4. Conclusion

Aminochelin-based 2,4-dinitrobenzenesulfonamide conjugate **2**, and three related analogues have been successfully synthesized. Rapid SO_2 release from the conjugates is observed on reaction with glutathione. The presence of a siderophore unit does not significantly impact the SO_2

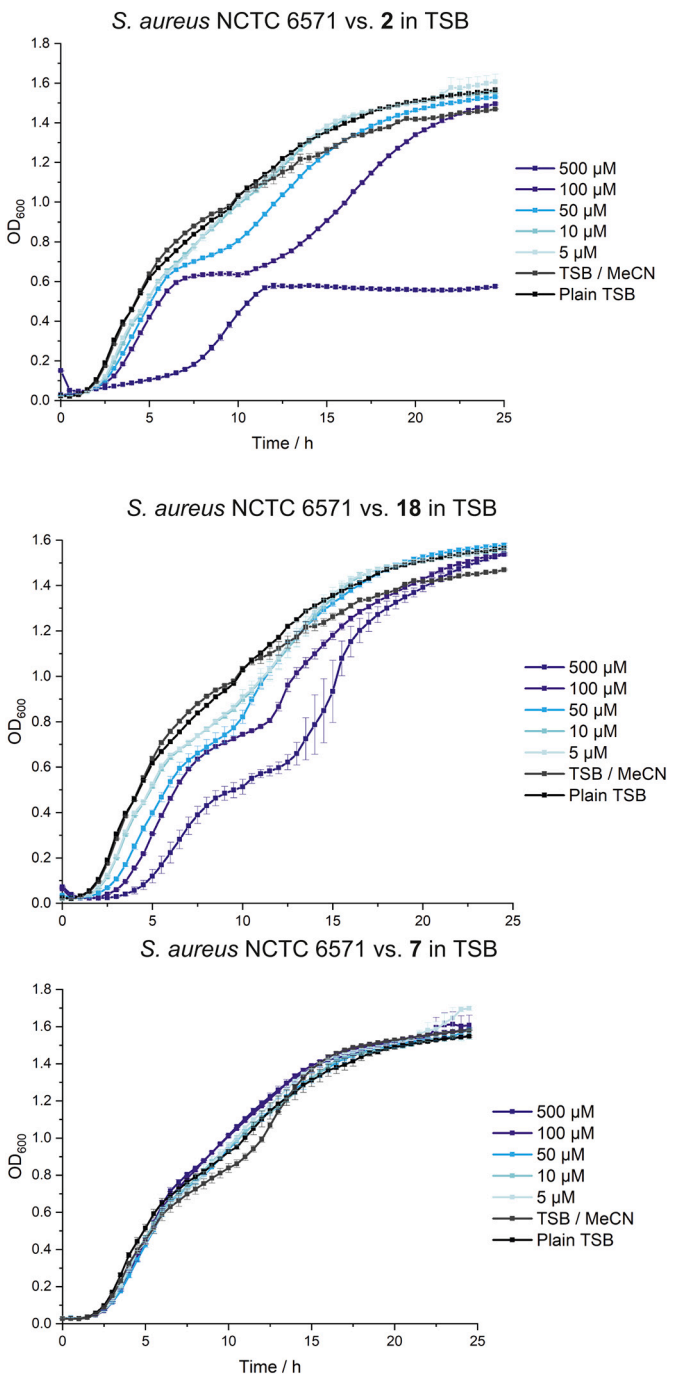

Fig. 7. Growth curves for selected concentrations of **2**, **7** and **18** *vs. S. aureus* in TSB. Results for **2** and **18** were presented as means of triplicate wells, and **7** as means of duplicate wells. Error bars were calculated as the standard error of the average.

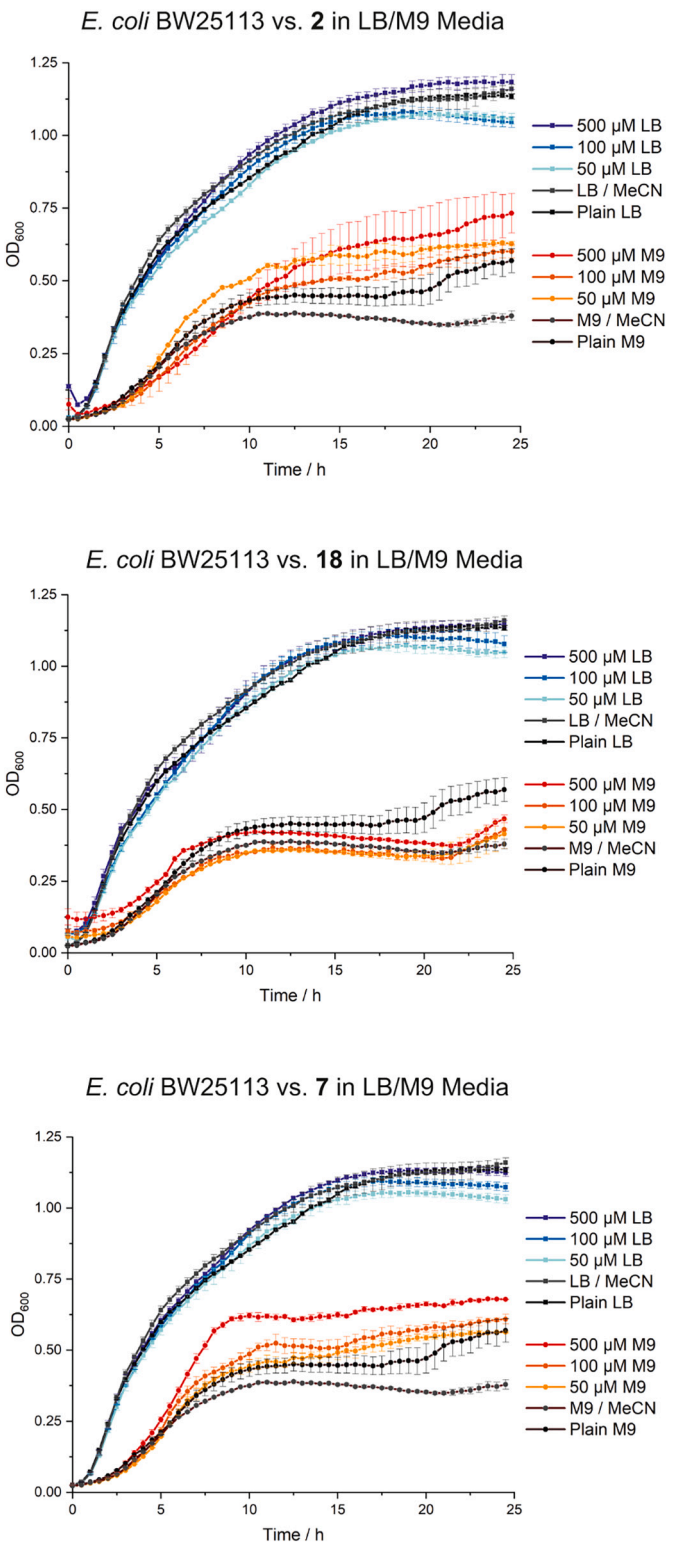

Fig. 8. Growth curves for selected concentrations of **2**, **7** and **18** *vs. E. coli* in both LB media (blue, squares) and M9 media (red, circles). Results were presented as means of duplicate wells. Error bars were calculated as the standard error of the average. (For interpretation of the references to color in this figure legend, the reader is referred to the web version of this article.)

release rate for **2** compared to prodrug **1**, although **5**, containing a shorter linker between the siderophore unit and the sulfonamide, sees a reduced rate of SO_2 release. The formation of Fe(III) conjugates was shown to accelerate the rate of SO_2 release. Compound **2** proved more active than "original" SO_2-releasing prodrug **18** against *S. aureus*, potentially indicating increased uptake facilitated by the aminochelin component. However, it is only active at high micromolar concentrations, and as with prodrug **18** proved inactive against wild-type *E. coli*. Reasonable antimicrobial activity could be observed for **2** in certain conditions against an *entA* mutant of *E. coli* unable to produce its own siderophores, suggesting the lack of activity of **2** *vs.* wild-type *E. coli* stems from an inability to compete with native siderophores for iron binding, which is required for uptake *via* siderophore transport pathways. In the future, the use of stronger iron-binding siderophore units like the hexadentate hydroxamate desferrioxamine B, or bis/tris

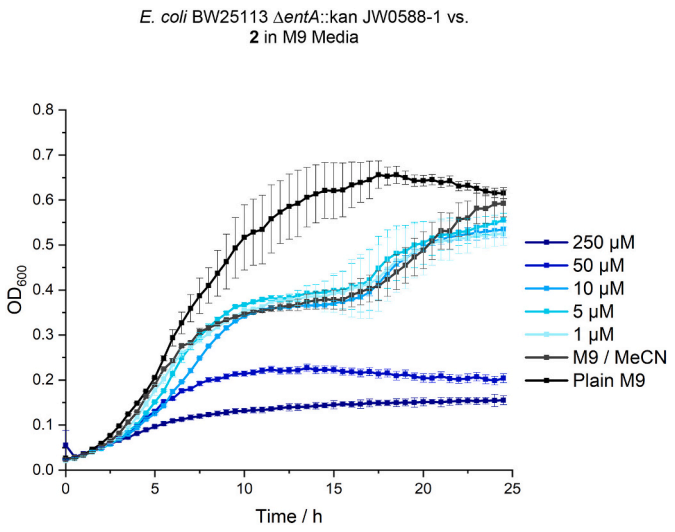

Fig. 9. Growth curves for concentrations of **2** *vs. E. coli entA* mutant in plain M9 media. Experiments are an average of two wells, with the exception of the M9 controls, which are an average of three wells. Error bars are calculated as the standard error of the mean.

(catecholate) siderophores, such as enterobactin, may offer improved uptake, and a subsequent boost to antimicrobial activity. The ability of siderophores to deliver SO_2-releasing prodrugs into bacteria, as demonstrated here, may also offer a new avenue in the development of Trojan Horse conjugates capable of cytoplasmic drug release, especially if the prodrugs can be tailored to achieve concurrent release of another antimicrobial unit, as demonstrated by Chakrapani and colleagues in 2019. [48] Exploration of this area and further mutant studies are ongoing.

CRediT authorship contribution statement

Conor M. Black: Conceptualization, Investigation, Methodology, Writing – original draft, Writing – review & editing. **Adrian J. Chu:** Investigation, Methodology, Writing – review & editing. **Gavin H. Thomas:** Supervision, Funding acquisition, Writing – review & editing. **Anne Routledge:** Conceptualization, Supervision, Funding acquisition, Writing – review & editing. **Anne-Kathrin Duhme-Klair:** Conceptualization, Supervision, Project administration, Funding acquisition, Writing – review & editing.

Declaration of Competing Interest

The authors declare that they have no known competing financial interests or personal relationships that could have appeared to influence the work reported in this paper.

Acknowledgements

We thank the UK Engineering and Physical Research Council (EPSRC) for a studentship for CMB [EP/N509802/1]. The work was part-funded by the Wellcome Trust [ref: 204829] through the 'Centre for Future Health (CFH) at the University of York'. In addition, A.-K. D.-K. acknowledges EPSRC grants EP/T007338/1 and EP/L024829/1. We thank Heather Fish for her assistance in obtaining NMR spectra and Karl Heaton for assistance in acquiring MS data.

Appendix A. Supplementary data

Supplementary data to this article can be found online at https://doi.org/10.1016/j.jinorgbio.2022.111875.

References

[1] S.C. Davies, T. Fowler, J. Watson, D.M. Livermore, D. Walker, Annual Report of the Chief Medical Officer: infection and the rise of antimicrobial resistance, Lancet (London, England) 381 (2013) 1606–1609, https://doi.org/10.1016/S0140-6736(13)60604-2.
[2] Y.Y. Liu, Y. Wang, T.R. Walsh, L.X. Yi, R. Zhang, J. Spencer, Y. Doi, G. Tian, B. Dong, X. Huang, L.F. Yu, D. Gu, H. Ren, X. Chen, L. Lv, D. He, H. Zhou, Z. Liang, J.H. Liu, J. Shen, Emergence of plasmid-mediated colistin resistance mechanism MCR-1 in animals and human beings in China: a microbiological and molecular biological study, Lancet Infect. Dis. 16 (2016) 161–168, https://doi.org/10.1016/S1473-3099(15)00424-7.
[3] R.J. Melander, C. Melander, The challenge of overcoming antibiotic resistance: an adjuvant approach? ACS Infect. Dis. 3 (2017) 559–563, https://doi.org/10.1021/acsinfecdis.7b00071.
[4] M.I. Hutchings, A.W. Truman, B. Wilkinson, Antibiotics: past, present and future, Curr. Opin. Microbiol. 51 (2019) 72–80, https://doi.org/10.1016/j.mib.2019.10.008.
[5] Antibacterial Agents in Clinical Development, Geneva, 2020.
[6] D.O. Schairer, J.S. Chouake, J.D. Nosanchuk, A.J. Friedman, The potential of nitric oxide releasing therapies as antimicrobial agents, Virulence. 3 (2012) 271–279, https://doi.org/10.4161/viru.20328.
[7] A.W. Carpenter, M.H. Schoenfisch, Nitric oxide release: part II. Therapeutic applications, Chem. Soc. Rev. 41 (2012) 3742–3752, https://doi.org/10.1039/C2CS15273H.
[8] L.S. Nobre, J.D. Seixas, C.C. Romão, L.M. Saraiva, Antimicrobial action of carbon monoxide-releasing compounds, Antimicrob. Agents Chemother. 51 (2007) 4303–4307, https://doi.org/10.1128/AAC.00802-07.
[9] J. Cheng, J. Hu, Recent advances on carbon monoxide releasing molecules for antibacterial applications, ChemMedChem. 16 (2021) 3628–3634, https://doi.org/10.1002/cmdc.202100555.
[10] R. Singh, U. Manjunatha, H.I.M. Boshoff, Y.H. Ha, P. Niyomrattanakit, R. Ledwidge, C.S. Dowd, I.Y. Lee, P. Kim, L. Zhang, S. Kang, T.H. Keller, J. Jiricek, C.E. Barry 3rd, PA-824 Kills nonreplicating *Mycobacterium tuberculosis* by intracellular NO release, Science 322 (2008) 1392–1395, https://doi.org/10.1126/science.1164571.
[11] P. Henderson, Sulfur Dioxide: science behind this anti-microbial, anti-oxidant, wine additive, Pract. Winer. Vineyard J. (2009) 1–6, https://doi.org/10.1016/B978-0-08-011432-3.50007-1.
[12] R.F. Guerrero, E. Cantos-Villar, Demonstrating the efficiency of Sulphur dioxide replacements in wine: a parameter review, Trends Food Sci. Technol. 42 (2015) 27–43, https://doi.org/10.1016/j.tifs.2014.11.004.
[13] S.R. Malwal, D. Sriram, P. Yogeeswari, V.B. Konkimalla, H. Chakrapani, Design, synthesis, and evaluation of thiol-activated sources of sulfur dioxide (SO 2) as antimycobacterial agents, J. Med. Chem. 55 (2012) 553–557, https://doi.org/10.1021/jm201023g.
[14] S.R. Malwal, D. Sriram, P. Yogeeswari, H. Chakrapani, Synthesis and antimycobacterial activity of prodrugs of sulfur dioxide (SO2), Bioorg. Med. Chem. Lett. 22 (2012) 3603–3606, https://doi.org/10.1016/j.bmcl.2012.04.048.
[15] K.A. Pardeshi, S.R. Malwal, A. Banerjee, S. Lahiri, R. Rangarajan, H. Chakrapani, Thiol activated prodrugs of sulfur dioxide (SO2) as MRSA inhibitors, Bioorg. Med. Chem. Lett. 25 (2015) 2694–2697, https://doi.org/10.1016/j.bmcl.2015.04.046.
[16] C.R.H. Raetz, C. Whitfield, Lipopolysaccharide Endotoxins, Annu. Rev. Biochem. 71 (2002) 635–700, https://doi.org/10.1146/annurev.biochem.71.110601.135414.
[17] H. Nikaido, Molecular basis of bacterial outer membrane permeability revisited, Microbiol. Mol. Biol. Rev. 67 (2003) 593–656, https://doi.org/10.1128/MMBR.67.4.593-656.2003.
[18] A.H. Delcour, Outer membrane permeability and antibiotic resistance, Biochim. Biophys. Acta - proteins, Proteomics. 1794 (2009) 808–816, https://doi.org/10.1016/j.bbapap.2008.11.005.
[19] J. Wang, W. Ma, X. Wang, Insights into the structure of *Escherichia coli* outer membrane as the target for engineering microbial cell factories, Microb. Cell Factories 20 (2021) 73, https://doi.org/10.1186/s12934-021-01565-8.
[20] I.J. Schalk, G.L.A. Mislin, Bacterial Iron uptake pathways: gates for the import of bactericide compounds, J. Med. Chem. 60 (2017) 4573–4576, https://doi.org/10.1021/acs.jmedchem.7b00554.
[21] P. Klahn, M. Brönstrup, Bifunctional antimicrobial conjugates and hybrid antimicrobials, Nat. Prod. Rep. 34 (2017) 832–885, https://doi.org/10.1039/C7NP00006E.
[22] K.H. Negash, J.K.S. Norris, J.T. Hodgkinson, Siderophore–antibiotic conjugate design: new drugs for bad bugs? Molecules. 24 (2019) 3314, https://doi.org/10.3390/molecules24183314.
[23] Y.-M. Lin, M. Ghosh, P.A. Miller, U. Möllmann, M.J. Miller, Synthetic sideromycins (skepticism and optimism): selective generation of either broad or narrow spectrum Gram-negative antibiotics, BioMetals. 32 (2019) 425–451, https://doi.org/10.1007/s10534-019-00192-6.
[24] M.G.P. Page, The role of Iron and Siderophores in infection, and the development of Siderophore antibiotics, Clin. Infect. Dis. 69 (2019) S529–S537, https://doi.org/10.1093/cid/ciz825.
[25] H. Kong, W. Cheng, H. Wei, Y. Yuan, Z. Yang, X. Zhang, An overview of recent progress in siderophore-antibiotic conjugates, Eur. J. Med. Chem. 182 (2019), 111615, https://doi.org/10.1016/j.ejmech.2019.111615.
[26] M.J. Miller, R. Liu, Design and syntheses of new antibiotics inspired by Nature's quest for Iron in an oxidative climate, Acc. Chem. Res. 54 (2021) 1646–1661, https://doi.org/10.1021/acs.accounts.1c00004.

[27] A. Sargun, R.R. Gerner, M. Raffatellu, E.M. Nolan, Harnessing Iron acquisition machinery to target Enterobacteriaceae, J. Infect. Dis. 223 (2021) S307–S313, https://doi.org/10.1093/infdis/jiaa440.
[28] A. Pandey, E. Boros, Coordination complexes to combat bacterial infections: recent developments, current directions and future opportunities, Chem. – A Eur. J. 27 (2021) 7340–7350, https://doi.org/10.1002/chem.202004822.
[29] W.H. Rastetter, T.J. Erickson, M.C. Venuti, Synthesis of iron chelators. Enterobactin, enantioenterobactin, and a chiral analog, J. Organomet. Chem. 46 (1981) 3579–3590, https://doi.org/10.1021/jo00331a001.
[30] A.-K. Duhme, R.C. Hider, H.H. Khodr, Synthesis and Iron-binding properties of Protochelin, the Tris(catecholamide) Siderophore of *Azotobacter vinelandii*, Chem. Ber. Recl. 130 (1997) 969–973.
[31] S. Lei, B. Jin, Q. Zhang, Z. Zhang, X. Wang, R. Peng, S. Chu, Synthesis of bifunctional biscatecholamine chelators for uranium decorporation, Polyhedron. 119 (2016) 387–395, https://doi.org/10.1016/j.poly.2016.09.006.
[32] K. Pappas, X. Zhang, W. Tang, S. Fang, Phenyl esters, preferred reagents for mono-acylation of polyamines in the presence of water, Tetrahedron Lett. 50 (2009) 5741–5743, https://doi.org/10.1016/j.tetlet.2009.07.142.
[33] A. Ito, T. Sato, M. Ota, M. Takemura, T. Nishikawa, S. Toba, N. Kohira, S. Miyagawa, N. Ishibashi, S. Matsumoto, R. Nakamura, M. Tsuji, Y. Yamano, In vitro antibacterial properties of Cefiderocol, a novel Siderophore cephalosporin, against gram-negative Bacteria, Antimicrob. Agents Chemother. 62 (2018), e01454-17, https://doi.org/10.1128/AAC.01454-17.
[34] G.G. Zhanel, A.R. Golden, S. Zelenitsky, K. Wiebe, C.K. Lawrence, H.J. Adam, T. Idowu, R. Domalaon, F. Schweizer, M.A. Zhanel, P.R.S. Lagacé-Wiens, A. J. Walkty, A. Noreddin, J.P. Lynch III, J.A. Karlowsky, Cefiderocol: a Siderophore cephalosporin with activity against Carbapenem-resistant and multidrug-resistant gram-negative Bacilli, Drugs. 79 (2019) 271–289, https://doi.org/10.1007/s40265-019-1055-2.
[35] J.Y. Wu, P. Srinivas, J.M. Pogue, Cefiderocol: a novel agent for the management of multidrug-resistant gram-negative organisms, Infect. Dis. Ther. 9 (2020) 17–40, https://doi.org/10.1007/s40121-020-00286-6.
[36] A. Souto, M.A. Montaos, M. Balado, C.R. Osorio, J. Rodríguez, M.L. Lemos, C. Jiménez, Synthesis and antibacterial activity of conjugates between norfloxacin and analogues of the siderophore vanchrobactin, Bioorg. Med. Chem. 21 (2013) 295–302, https://doi.org/10.1016/j.bmc.2012.10.028.
[37] A. Paulen, V. Gasser, F. Hoegy, Q. Perraud, B. Pesset, I.J. Schalk, G.L.A. Mislin, Synthesis and antibiotic activity of oxazolidinone-catechol conjugates against *Pseudomonas aeruginosa*, Org. Biomol. Chem. 13 (2015) 11567–11579, https://doi.org/10.1039/c5ob01859e.
[38] A.J. Cohen, J.N. Smith, Comparative Detoxication. 9. Metabolism of some halogenated compounds by conjugation with glutathione in the locust, Biochem. J. 90 (1964) 449.
[39] I. Mancini, G. Guella, G. Chiasera, F. Pietra, Glutathione S-transferase catalysed dehalogenation of haloaromatic compounds which lack nitro groups near the reaction Centre, Tetrahedron Lett. 39 (1998) 1611–1614, https://doi.org/10.1016/S0040-4039(97)10830-9.
[40] D.M. Missiakas, O. Schneewind, Growth and laboratory maintenance of *Staphylococcus aureus*, in: Curr. Protoc. Microbiol., 2013, https://doi.org/10.1002/9780471729259.mc09c01s28. Chapter 9. Unit-9C.1.
[41] M.H. Zwietering, I. Jongenburger, F.M. Rombouts, K. van Riet, Modeling of the bacterial growth curve, Appl. Environ. Microbiol. 56 (1990) 1875–1881, https://doi.org/10.1128/aem.56.6.1875-1881.1990.
[42] D. Chu, D.J. Barnes, The lag-phase during diauxic growth is a trade-off between fast adaptation and high growth rate, Sci. Rep. 6 (2016) 25191, https://doi.org/10.1038/srep25191.
[43] A. Brauner, O. Fridman, O. Gefen, N.Q. Balaban, Distinguishing between resistance, tolerance and persistence to antibiotic treatment, Nat. Rev. Microbiol. 14 (2016) 320–330, https://doi.org/10.1038/nrmicro.2016.34.
[44] A.-A.D. Jones, D. Medina-Cruz, N.Y. Kim, G. Mi, C. Bartomeu-Garcia, L. Baranda-Pellejero, N. Bassous, T.J. Webster, Statistical classification of dynamic bacterial growth with sub-inhibitory concentrations of nanoparticles and its implications for disease treatment, BioRxiv. (2020), https://doi.org/10.1101/2020.07.19.210930.
[45] S.C. Andrews, A.K. Robinson, F. Rodriguez-Quinones, Bacterial iron homeostasis, FEMS Microbiol. Rev. 27 (2003) 215–237, https://doi.org/10.1016/S0168-6445(03)00055-X.
[46] J. Liu, K. Duncan, C.T. Walsh, Nucleotide sequence of a cluster of *Escherichia coli* enterobactin biosynthesis genes: identification of entA and purification of its Nucleotide Sequence of a Cluster of *Escherichia coli* Enterobactin Biosynthesis Genes: identification of entA and Purific, J. Bacteriol. 791–798 (1989).
[47] M. Sakaitani, F. Rusnak, N.R. Quinn, C. Tu, T.B. Frigo, G.A. Berchtold, C.T. Walsh, Mechanistic studies on trans-2,3-Dihydro-2,3-dihydroxybenzoate dehydrogenase (Ent A) in the biosynthesis of the Iron Chelator Enterobactin, Biochemistry. 29 (1990) 6789–6798, https://doi.org/10.1021/bi00481a006.
[48] K.A. Pardeshi, T.A. Kumar, G. Ravikumar, M. Shukla, G. Kaul, S. Chopra, H. Chakrapani, Targeted antibacterial activity guided by Bacteria-specific Nitroreductase catalytic activation to produce ciprofloxacin, Bioconjug. Chem. 30 (2019) 751–759, https://doi.org/10.1021/acs.bioconjchem.8b00887.